

Disturbance Observer Based Repetitive Control System with Non-minimal State-space Realization and Experimental Evaluation

Liuping Wang¹, Chris T. Freeman², Eric Rogers², and Peter C. Young³

Abstract—This paper develops a disturbance observer-based repetitive control system using a non-minimal state-space realization where all state variables correspond to the system's input and output variables and past values. Tracking a periodic reference signal or rejection of a periodic disturbance signal is achieved by including a disturbance observer to estimate an input disturbance containing the same frequency characteristics. This new approach differs from previously published designs because it separates the design procedure into two tasks: first, stabilization via state feedback control; secondly, independent incorporation of the periodic modes via estimation of the disturbance. Moreover, the new design naturally contains an anti-windup mechanism when the control signal reaches its maximum or minimum value. Results from the experimental evaluation are given, including a comparison against a design that constructs a minimal state controller using an observer. These results demonstrate that the new method can deliver significant performance improvement, with excellent disturbance rejection and reference tracking.

Index Terms—repetitive control, non-minimal state-space realization, disturbance observer, disturbance rejection, anti-windup mechanism, experimental validation.

I. INTRODUCTION

Two types of representations arise in control engineering applications based on dynamic models. One is the class of physical models, such as those for electrical machines and power converters, which result from the application of physical laws, and the other is by system identification, see, e.g., [1], [2], [3]. The second type of model is often given in the transfer-function form and arises in, e.g., electro-mechanical systems and chemical process control.

Suppose the state variables are not (or cannot be) measured for state feedback control. In that case, it is a common practice to use an observer to estimate the state variables (or those not directly available). In transfer-function models, the state variables are not known unless they correspond to the sets of input and output variables. This latter case is the setting for non-minimal state-space (NMSS) feedback control. See, e.g., [4], [5]. The non-minimal state-space realization can be used in the design of model predictive controllers, see, e.g., [6], [7]. Advantages arising from the use of NMSS state feedback control include no need for observer-based implementation.

Hence, faster closed-loop response to disturbance rejection and better performance for reference following (or tracking).

The main objective of this paper is to show that repetitive control systems design can be enhanced by using an NMSS model based on full state feedback control. In particular, it considers repetitive control systems that can track a multi-frequency periodic reference signal or reject the same type of disturbance signal. These objectives, by the internal model control principle [8] require that the characteristics of the reference signal or the disturbance, as appropriate, are embedded in the control structure used.

In contrast to other repetitive predictive designs, the new design estimates the periodic disturbance signal using a suitably structured observer and subtracts it from an optimized control signal. This type of approach is known as disturbance observer-based control in the literature. Disturbance observer-based linear and nonlinear control systems can be found in, e.g., [9], [10], [11], [12].

The early work on motion control using disturbance observer includes [13]. A disturbance observer applied to rigid mechanical systems is described in [14] and a robotic manipulator in [15]. Controller design for disturbance rejection using a disturbance observer with frequency estimation is the subject in [16]. Stability and robust performance of motion control systems that use a disturbance observer are analyzed in, e.g., [17].

In [18], similar approaches for engine-induced vibration are the subject, based on estimating sinusoidal disturbances and canceling them. An adaptive frequency estimation method, together with a traditional disturbance observer, is used in [16], [19] to estimate the disturbance frequency online. A transfer-function-based approach using a disturbance observer for controlling magnetic disk drives is reported in [20]. Moreover, a similar approach, together with the online estimation of disturbance frequency, is described in [21]. More recent applications of disturbance observer in the area of power electronics are described in [23] and [24].

This paper addresses the following interrelated design issues.

- 1) How to design a disturbance observer to produce a repetitive control system that will naturally embed the periodic modes identified from the reference and/or disturbance signal(s).
- 2) The development of an NMSS representation of the dynamics and reducing the number of estimated variables leads to simplicity in the design and implementation.

¹School of Engineering, RMIT University, Australia. Email: liuping.wang@rmit.edu.au

²School of Electronics and Computer Science, University of Southampton, UK. Email: {cf, etar}@ecs.soton.ac.uk

³Lancaster Environment Centre and Data science Institute, University of Lancaster, UK. Email: p.young@lancaster.ac.uk

Equally crucial for applications is that the disturbance observer naturally provides an anti-windup mechanism if the control signal reaches its operational limits. Experimental validation results on one axis of a gantry robot are given, together with experimental comparison against a design based on a minimal state-space realization and the use of an observer for implementation.

II. DISTURBANCE OBSERVER BASED REPETITIVE CONTROL

A. Mathematical Model

This paper considers single-input single-output discrete linear systems described by the difference equation:

$$\begin{aligned} y(k+1) &= -a_1y(k) - a_2y(k-1) \dots - a_ny(k-n) \\ &+ b_1u(k) + b_2u(k-1) + \dots + b_nu(k-n) \end{aligned} \quad (1)$$

where $u(k)$ and $y(k)$ are the input and output variables. The model coefficients a_1, a_2, \dots, a_n and b_1, b_2, \dots, b_n are obtained either from system identification or mathematical modeling.

Given a periodic reference signal $r(k)$, the error between the output and the reference signal is defined as

$$e(k) = y(k) - r(k)$$

The disturbance observer approach first designs a suitably structured observer (that nullifies the effects of the reference and/or the disturbance) and then combines it with a stabilizing controller. Denoting the observer output by $\hat{\mu}(k)$, the control input $u(k)$ is given by

$$u(k) = \tilde{u}(k) - \hat{\mu}(k) \quad (2)$$

where $\tilde{u}(k)$ is the optimized control signal and (as one option) taken as state feedback designed using a linear quadratic regulator setting. Combining these equations with the observer characteristics gives the following discrete-time model linking input \tilde{u} and the error signal e

$$\begin{aligned} e(k+1) &= -a_1e(k) - a_2e(k-1) \dots - a_n e(k-n) \\ &+ b_1\tilde{u}(k) + b_2\tilde{u}(k-1) + \dots + b_n\tilde{u}(k-n) \end{aligned} \quad (3)$$

To convert this model to state-space form, the state variables are selected as the input and the output signals, including their relevant past values, i.e.,

$$x(k) = [e(k) \quad \dots \quad e(k-n) \quad \tilde{u}(k-1) \quad \dots \quad \tilde{u}(k-n)]^T$$

The non-minimal state-space representation of (3) can now be written as:

$$\begin{aligned} x(k+1) &= A_mx(k) + B_m\tilde{u}(k) \\ e(k) &= C_mx(k) \end{aligned} \quad (4)$$

where the matrices A_m and B_m are

$$A_m = \begin{bmatrix} -a_1 & -a_2 & \dots & b_2 & \dots & b_n \\ 1 & 0 & 0 & 0 & 0 & 0 \\ 0 & \ddots & 0 & 0 & 0 & 0 \\ 0 & 0 & 1 & 0 & 0 & 0 \\ 0 & 0 & 0 & 0 & 0 & 0 \\ 0 & 0 & \dots & 1 & \dots & 0 \\ \vdots & \vdots & \ddots & 0 & \ddots & 0 \\ 0 & 0 & \dots & 0 & 1 & 0 \end{bmatrix}, \quad B_m = \begin{bmatrix} b_1 \\ 0 \\ \vdots \\ 0 \\ 1 \\ 0 \\ \vdots \\ 0 \end{bmatrix}$$

$$C_m = [1 \quad 0 \quad 0 \quad \dots \quad 0 \quad 0]$$

The repetitive control system design consists of a state feedback controller, with gain matrix K chosen such that:

$$x(k+1) = (A_m - B_mK)x(k)$$

is stable, i.e., all eigenvalues of $A_m - B_mK$ have modulus strictly less than one. Under the action of this control law, the intermediate control signal is

$$\tilde{u}(k) = -Kx(k)$$

Moreover, $\mu(k)$ is estimated by an observer structure developed in the next section and the control signal is

$$u(k) = \tilde{u}(k) - \hat{\mu}(k)$$

Figure 1 gives a block diagram representation of the control scheme for implementation.

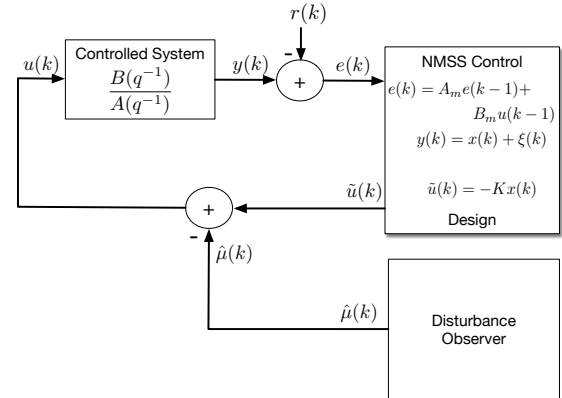


Fig. 1: The scheme for implementation.

B. Disturbance Observer

To estimate the periodic input disturbance, $\hat{\mu}(k)$ assuming that all entries of the state vector $x(k)$ are measured, the method followed is from [25]. In particular, it is assumed that either the reference signal $r(k)$ and/or the input disturbance signal $\mu(k)$ have been analyzed to obtain the dominant frequency components. Then these components can be modeled by a polynomial $D(q^{-1})$, where q^{-1} denotes the backward shift operator.

The input disturbance signal $\mu(k)$ is expressed in the form:

$$\mu(k) = \frac{\epsilon(k-1)}{D(q^{-1})} \quad (5)$$

where $\epsilon(k)$ is a zero-mean white noise sequence. Moreover, all roots of the polynomial $D(q^{-1})$ lie on the unit circle, which follows from frequency analysis of the reference signal and/or the disturbance signal. For example, if the reference signal is sinusoidal with N samples, then

$$D(q^{-1}) = 1 - 2 \cos \frac{2\pi}{N} q^{-1} + q^{-2}$$

In general, it is assumed that the $D(q^{-1})$ has order n_d and is written as

$$D(q^{-1}) = 1 + d_1 q^{-1} + d_2 q^{-2} + \dots + d_{n_d} q^{-n_d} \quad (6)$$

where the coefficients d_1, d_2, \dots, d_{n_d} are known.

Given the definition of the input disturbance (2) and the state-space model (4), it follows that the input disturbance $\mu(k)$ satisfies:

$$B_m \mu(k) = x(k+1) - A_m x(k) - B_m u(k) \quad (7)$$

Multiplying across this last equation from the left by the measurement matrix C_m gives

$$\begin{aligned} C_m B_m \mu(k) &= C_m x(k+1) - C_m A_m x(k) - C_m B_m u(k) \\ &= e(k+1) - C_m A_m x(k) - C_m B_m u(k) \end{aligned} \quad (8)$$

One way to reconstruct the input periodic disturbance $\mu(k)$ is to start from (8). However, this would not be sufficiently accurate to generate the repetitive control signal because of the uncertainties in the mathematical model and the requirement for access to the feedback error $e(k+1)$ at the current time k . Consequently, an observer to estimate $\mu(k)$ based on the disturbance model (5) is required.

Rewrite (5) in the difference equation form:

$$\mu(k+1) = -d_1 \mu(k) - d_2 \mu(k-1) - \dots - d_{n_d} \mu(k-n_d) + \epsilon(k) \quad (9)$$

and then the state vector $p(k)$ can be formed as

$$p(k) = [\mu(k) \quad \mu(k-1) \quad \dots \quad \mu(k-n_d)]^T$$

Hence a state-space model describing the dynamics of the disturbance has the form

$$\begin{aligned} p(k+1) &= A_d p(k) + B_d \epsilon(k) \\ \mu(k) &= C_d p(k) \end{aligned} \quad (10)$$

where

$$A_d = \begin{bmatrix} -d_1 & -d_2 & \dots & \dots & -d_{n_d} \\ 1 & 0 & \dots & \dots & 0 \\ 0 & 1 & 0 & \dots & 0 \\ \dots & \dots & \dots & \dots & \dots \\ 0 & 0 & \dots & 1 & 0 \end{bmatrix} \quad B_d = \begin{bmatrix} 1 \\ 0 \\ \vdots \\ \vdots \\ 0 \end{bmatrix}$$

$$C_d = [1 \quad 0 \quad \dots]$$

The measurement of the disturbance is $C_m B_m \mu(k)$, based on the right-hand side of (8) and with the assumption that $C_m B_m \neq 0$, the pair $\{A_d, C_m B_m C_d\}$ is observable. This

construction is a disturbance observer for the estimation of $p(k)$ given by

$$\begin{aligned} \hat{p}(k+1) &= A_d \hat{p}(k) + K_{ob}(C_m B_m \mu(k) - C_m B_m C_d \hat{p}(k)) \\ &= A_d \hat{p}(k) + K_{ob}(e(k+1) - C_m A_m x(k) \\ &\quad - C_m B_m u(k) - C_m B_m C_d \hat{p}(k)) \end{aligned} \quad (11)$$

where the observer gain K_{ob} is chosen based on the pair $(A_d, C_m B_m C_d)$ such that the observer error system is stable. Also, the observer error system is

$$\tilde{p}(k+1) = (A_d - K_{ob} C_m B_m C_d) \tilde{p}(k) + B_d \epsilon(k) \quad (12)$$

where $\tilde{p}(k) = p(k) - \hat{p}(k)$.

This error system description is obtained by substituting (8) into (11) and then subtracting (11) from (10). The disturbance dynamics are of relatively low order because the use of the non-minimal state-space model avoids the estimation of the state variables. This feature is significant when the system model is of a high order.

In the form (11), the disturbance observer is not implementable because the right-hand side involves the feedback error at $k+1$. Hence the intermediate variable $\hat{q}(k) = \hat{p}(k) - K_{ob} e(k)$ is introduced and then, by moving the term $K_{ob} e(k+1)$ from the right-hand side to the left-hand side and re-grouping, the estimated intermediate variable in the disturbance observer is given by

$$\begin{aligned} \hat{q}(k+1) &= (A_d - K_{ob} C_m B_m C_d) \hat{q}(k) \\ &\quad + (A_d - K_{ob} C_m B_m C_d) K_{ob} e(k) \\ &\quad - K_{ob}(C_m A_m x(k) + C_m B_m u(k)) \end{aligned} \quad (13)$$

Given an initial state vector $\hat{q}(0)$ and the control signal $u(k)$, output signal $y(k)$ and the reference signal $r(k)$, (13) provides a real-time estimation of the disturbance signal $\hat{\mu}(k)$.

It is routine to show that the transfer-function of the new controller contains the disturbance model $D(z^{-1})$ in its denominator, in accordance with the internal model principle, leading to infinite gains at the discrete frequencies where $D(z^{-1}) = 0$. In effect, this means that the (modulus of) the complementary sensitivity function $|T(e^{j\omega})| = \frac{G(e^{j\omega})C(e^{j\omega})}{1+G(e^{j\omega})C(e^{j\omega})}$ equals 1 for the frequencies corresponding to $D(q^{-1}) = 0$, where $G(e^{j\omega})$ and $C(e^{j\omega})$ denote the frequency responses of the model and the repetitive controller.

Consider also the case when the system uncertainty is quantified with the multiplicative modelling error $\Delta G_m(e^{j\omega}) = \frac{G^{true}(e^{j\omega}) - G(e^{j\omega})}{G(e^{j\omega})}$. Then by robust control theory, the sufficient condition to guarantee closed-loop stability in this case is $|T(e^{j\omega})| |G_m(e^{j\omega})| < 1$ for all ω . This requirement implies a repetitive control system demands higher model accuracy to ensure that $|\Delta G_m(e^{j\omega})| < 1$ for the frequency band that contains the frequencies used in the repetitive control system design.

III. IMPLEMENTATION OF THE REPETITIVE CONTROL SYSTEM WITH ANTI-WINDUP MECHANISM

Implementation of the control system designed in the previous section has a naturally occurring anti-windup mechanism when the control signal reaches its operational limits. This

property is present because the sinusoidal modes embedded in the repetitive control system arise through the estimation, which is a stable realization (see (13)) of the disturbance model.

For the implementation of the repetitive control system with its anti-windup mechanism, it is assumed that the control signal is constrained such that

$$u^{min} \leq u(k) \leq u^{max}$$

At the initial stage, the current and past control signal and output signal are known, and therefore the initial state vector $x(0)$ is given, and the initial state and $\hat{q}(0)$ is to be chosen. The following steps summarize the resulting computational algorithm.

- 1) Compute the estimated input disturbance:

$$\hat{p}(k) = \hat{q}(k) + K_{ob}e(k); \quad \hat{\mu}(k) = C_d\hat{p}(k)$$

- 2) Compute the control signal by subtracting the estimated disturbance from the feedback control law:

$$u(k) = -Kx(k) - \hat{\mu}(k)$$

- 3) Implement the saturation limits on the control signal:

$$u(k)^{act} = \begin{cases} u^{min}, & \text{if } u(k) < u^{min} \\ u(k), & \text{if } u^{min} \leq u(k) \leq u^{max} \\ u^{max}, & \text{if } u(k) > u^{max} \end{cases}$$

- 4) Update the disturbance observer with the saturation information based on (13), with the control signal replaced by $u(k)^{act}$.
- 5) Send the control signal $u(k)^{act}$ to the actuator and return to Step 1 when the next sampling period begins.

IV. EXPERIMENTAL VALIDATION

This section experimentally applies the design of the previous section to the gantry robot shown in Figure 2, which replicates the ‘pick and place’ operation, commonly found in a variety of industrial applications, where the operations are in synchronization with a conveyor system. Previous experimental research has modeled the dynamics from experimental data.

A. Modelling and Control System Design

For modeling and control design purposes, this gantry robot can be treated as three single-input single-output systems (one for each axis). A model of the dynamics for controller design was obtained by independently modeling each robot’s axis using frequency response tests. In this section, the X -axis model is used, which is the following 7th-order transfer-function (with s denoting the Laplace transform variable)

$$\begin{aligned} G(s) &= G_1(s)G_2(s) \\ G_1(s) &= \frac{(s + 500.19)(s + 4.90 \times 10^5)}{(s(s + 69.74 \pm j459.75))} \\ G_2(s) &= \frac{(s + 10.99 \pm j169.93)(s + 5.29 \pm j106.86)}{(s + 10.69 \pm j141.62)(s + 12.00 \pm j79.10)} \end{aligned} \quad (14)$$



Fig. 2: The gantry robot.

Sampling at $\Delta t = 0.01$ secs with a zero-order hold gives the following z -transfer-function model:

$$G(z^{-1}) = \frac{B(z^{-1})}{A(z^{-1})} \quad (15)$$

where the polynomials $A(z^{-1})$ and $B(z^{-1})$ together with their coefficients are given below:

$$\begin{aligned} A(z^{-1}) &= 1 + a_1z^{-1} + a_2z^{-2} + a_3z^{-3} + a_4z^{-4} + a_5z^{-5} \\ &\quad + a_6z^{-6} + a_7z^{-7} \end{aligned}$$

$$\begin{aligned} B(z^{-1}) &= b_1z^{-1} + b_2z^{-2} + b_3z^{-3} + b_4z^{-4} + b_5z^{-5} \\ &\quad + b_6z^{-6} + b_7z^{-7} \end{aligned}$$

$b_1 = 0.5174$, $b_2 = -0.0108$, $b_3 = 0.2863$, $b_4 = 0.1053$, $b_5 = -0.0816$, $b_6 = 0.0081$, $b_7 = -0.0006$; $a_1 = -1.5314$, $a_2 = 0.9717$, $a_3 = -0.3821$, $a_4 = -0.0056$, $a_5 = -0.0557$, $a_6 = 0.0036$, $a_7 = -0.0005$.

The NMSS model is formed by choosing the measured input and output variables as the state variables (see (3) and (4)). In this case, although the dimension of the state vector is quite high at 13, the implementation of the state vector is performed by simply shifting the data vector in real-time to reduce the computational load.

1) *Controller Design:* The state feedback controller is designed using linear quadratic regulator theory with cost function:

$$J = \sum_{k=0}^{\infty} x^T(k)Qx(k) + \sum_{k=0}^{\infty} \tilde{u}^T(k)R\tilde{u}(k) \quad (16)$$

where Q is the compatibly dimensioned identity matrix and $R = 1$. Also, to have a prescribed degree of stability [26], the closed-loop eigenvalues are required to lie within a circle of radius 0.97. Following [7], the MATLAB `dlqr` function was called in the following form:

$$K = \text{dlqr}(A_m/0.97, B_m/0.97, Q, R)$$

Figure 3 confirms that the resulting closed-loop eigenvalues are within the circle of radius 0.97.

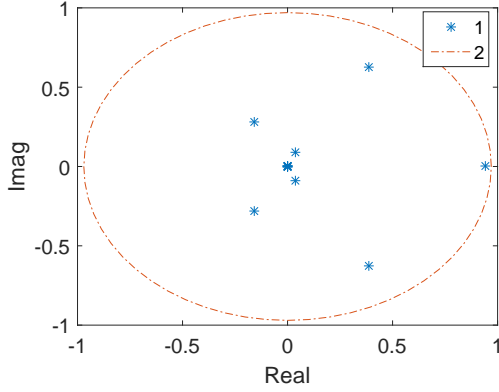


Fig. 3: The closed-loop eigenvalues of the state feedback control of NMSS. Key: (1) the eigenvalues; (2) the circle of radius 0.97.

2) *Disturbance Observer Design*: To design the disturbance observer, the model for $D(q^{-1})$ in (5) needs to be determined, which is linked to the actual application of the gantry robot. Figure 4 shows the desired trajectory of the robot movement used as an exemplar in this paper. This reference signal is

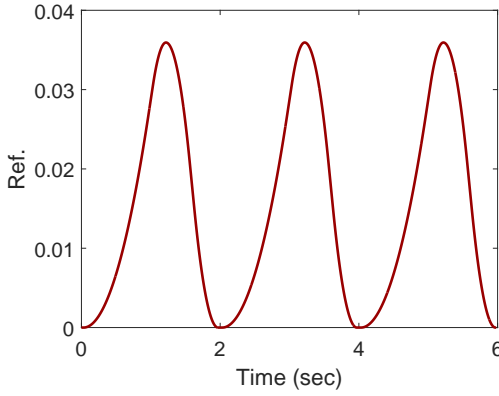


Fig. 4: The desired trajectory of the robotic arm.

periodic with the period $T = 2$ secs. Therefore, the fundamental frequency in continuous time is $\frac{2\pi}{T}$, which converts to the discrete time frequency $\frac{2\pi}{N}$ where $N = 200$ is the number of samples within one period. Clearly from Fig. 4, the DC component is seen and following earlier research [25], the polynomial $D(q^{-1})$ is chosen as

$$D(q^{-1}) = (1 - q^{-1})(1 - 2 \cos \frac{2\pi}{N} q^{-1} + q^{-2}) \quad (17)$$

The first term in $D(q^{-1})$ corresponds to the DC component, and the second to the dominant frequency in the reference signal. Given $D(q^{-1})$, the system matrix A_d in the state-space model follows from (10) as

$$A_d = \begin{bmatrix} 2.999 & -2.999 & 1 \\ 1 & 0 & 0 \\ 0 & 1 & 0 \end{bmatrix}$$

and the output matrix is

$$C_m B_m C_d = [0.5174 \times 10^{-3} \quad 0 \quad 0]$$

The MATLAB function `dlqr` is used again, this time to find the observer gain K_{ob} , where Q is the identity matrix and $R = 1$. Again, the closed-loop eigenvalues are required to be within the circle of radius 0.97, which results in:

$$K_{ob} = [582.4820 \quad 516.4691 \quad 453.6249]^T$$

and the closed-loop eigenvalues are $0.9138 \pm j0.0849$, 0.8699 . Since the eigenvalues of the A_d matrix lie on the unit circle of the complex plane, moving the closed-loop eigenvalues of the observer error system further towards the origin of the complex plane will lead to increased observer gains, which would further amplify the measurement noise in the system.

B. Experimental Evaluation

1) *Reference Tracking*: In the experiments, $x(0) = 0$ is assumed, and also that all the past values of the input and output signals are zero. Fig. 5, top plot, compares the output response $y(k)$ with the reference signal $r(k)$, where the reference signal is in blue and the output in red. The error signal $r(k) - y(k)$ is shown separately in Fig. 5, middle plot; and the required control signal is in Fig. 5, bottom plot. These figures confirm that the repetitive control system can deliver close reference signal tracking, despite the measurement noise. The mean square error between the reference and the output is

$$E = \frac{1}{M} \sum_{k=1}^M (r(k) - y(k))^2 = 1.5103 \times 10^{-6} \quad (18)$$

where M is the number of data points.

2) *Disturbance Rejection with Amplitude Constraints: Periodic Disturbance*: Disturbance rejection is a significant objective for repetitive control design. In this respect, the capability of the new design is examined by holding the robot arm in the initial location, i.e., zero reference signal, and injecting a periodic disturbance together with a random walk type of disturbance on the input. In particular, the disturbance $\mu(k)$ used in the experimental study is generated using the following equation:

$$\mu(k) = 10 \left(\sin\left(\frac{2\pi k}{300}\right) + \frac{0.01}{1 - 0.99q^{-1}} \epsilon(k) \right) \quad (19)$$

where $\epsilon(k)$ is normally distributed white noise with standard deviation 0.01. A mismatch between the frequencies in the designed repetitive controller and the disturbance is included to demonstrate that the repetitive control system is robust in this regard.

The first term in (19) represents the low-frequency sinusoidal disturbance, and the second a random walk disturbance. Also, there is measurement noise added to the position sensor of the robot. To demonstrate the effectiveness of the anti-windup mechanism in the design, the control signal is limited to ± 10 V.

Fig. 6, top plot, shows that the robot maintains the desired position despite the significant periodic and random walk disturbances, with variations within ± 0.006 . Fig. 6, bottom plot, gives the repetitive control signal used to reject the disturbance, which is limited to within the required amplitude. The results in these two figures are representatives of numerous experimental tests.

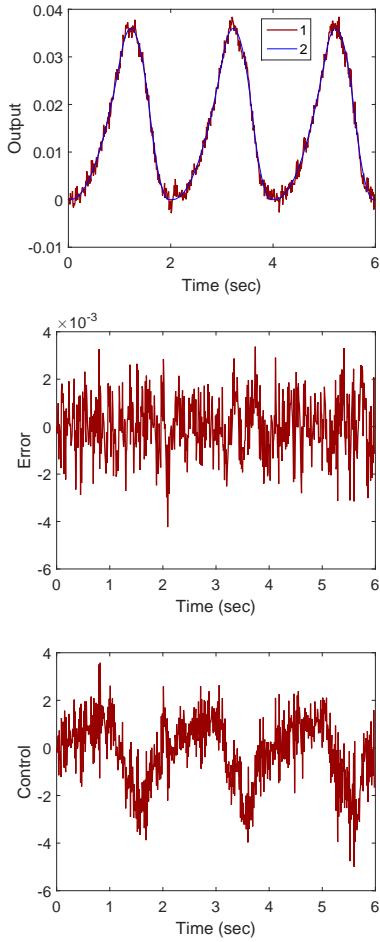


Fig. 5: experimental results. Top plot, output and reference signals, middle plot, the error and bottom plot the control signal..

V. COMPARATIVE STUDY

This section gives the results of a comparative study, including experimental validation, of the new design's performance and an alternative based on a minimal state-space realization of the model of dynamics of the X axis of the gantry robot. Again, both reference following (or tracking) and disturbance rejection are considered.

A. Minimal State-space Realization with Disturbance Observer

For a system model given by a transfer-function, an observer must estimate the state vector entries because they are not known in the general context of a minimal state-space realization. Assuming that $\mu(k)$ is present, the state-space model of the dynamics has the form:

$$\begin{aligned} x_p(k+1) &= A_p x_p(k) + B_p(u(k) + \mu(k)) \\ y(k) &= C_p x_p(k) \end{aligned} \quad (20)$$

where A_p , B_p and C_p are obtained by constructing a minimal realization of the 7th order transfer-function (14), followed by

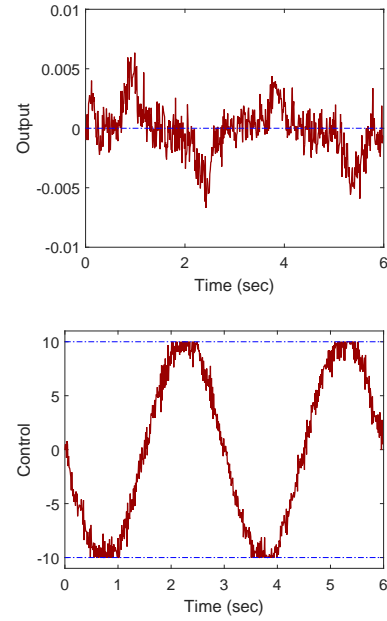


Fig. 6: Rejection of periodic and random walk disturbance with measurement noise with constraints – top plot, output, bottom plot, control signal.

discretization at $\Delta t = 0.01$ secs using a zero-order hold. The minimal state-space realization has state dimension 7.

To estimate $x_p(k)$ together with $\mu(k)$, introduce the state vector

$$z(k) = [x_p^T(k) \quad \mu(k) \quad \dots \quad \mu(k - n_d + 1)]^T$$

and hence the following augmented state-space model for the observer design

$$\begin{aligned} z(k+1) &= A_o z(k) + B_o u(k) + \bar{B}_o \epsilon(k) \\ y(k) &= C_o z(k) \end{aligned} \quad (21)$$

where

$$\begin{aligned} A_o &= \begin{bmatrix} A_p & \bar{B}_p \\ O & A_d \end{bmatrix}, \\ \bar{B}_p &= [B_p \quad O] \\ B_o &= \begin{bmatrix} B_p \\ O \end{bmatrix}; \quad \bar{B}_o = \begin{bmatrix} O \\ I \\ O \end{bmatrix} \\ C_o &= [C_p \quad O] \end{aligned}$$

and O and I , respectively, denote the null and identity matrices of compatible dimensions. Also the pair of matrices $\{A_o, C_o\}$ is observable provided the pair $\{A_p, C_p\}$ from (20) is observable.

The state feedback controller is designed using the pair $\{A_p, B_p\}$ and the MATLAB function `dlqr` produces the controller gain vector K_p , where in (16), applied to this case, $Q = I$, $R = 1$ and the closed-loop eigenvalues are constrained to lie within a circle of radius 0.97.

The minimal state feedback control law based on the above computations is:

$$u(k) = -K_p \hat{x}_p(k) - \hat{\mu}(k)$$

and $\hat{x}_p(k)$ and $\hat{\mu}(k)$ are estimated using the observer:

$$\hat{x}_o(k+1) = A_o \hat{x}_o(k) + B_o u(k) + K_{ob}(y(k) - r(k) - C_o \hat{x}_o(k))$$

where $r(k)$ is the reference signal and the number of states to be estimated is 10. The observer gain vector for the choice of $Q = I$ and $R = 1$, with the eigenvalues of the closed-loop error system constrained to lie inside the circle of radius 0.97, is computed using MATLAB function `dlqr`. This function is used in the following form:

$$K_{ob} = \text{dlqr}(A_o/0.97, C_o/0.97, Q, R)$$

resulting in the entries: 0.0005, 0.0001, -0.0001, 0.0050, 0.0028, 526, 166, 190, 180, 170.

In this case, poor numerical scaling of the observer gains is present compared to the NMSS based design. Also, it is quite difficult to design the higher-order observer, which is why the prescribed degree of stability approach [26] has been used.

B. Experimental Evaluation

The performance of the design with that of the previous section is compared under the same experimental conditions for both, i.e., the reference and disturbance signals, the measurement noise, and the initial conditions of the robotic arm. The closed-loop error between the reference signal $r(k)$ and the output of the repetitive control system $y(k)$ designed in this section is

$$e(k) = r(k) - y(k)$$

Figs. 7–9 gives corresponding experimental results, where for each case, the red line is the minimal realization and the dashed black line the NMSS. Figure 7 compares the errors for reference tracking without constraints, and the design of this section has some difficulties in smoothly tracking the reference signal. Figure 8 gives the errors for sinusoidal disturbance rejection. These experimental results show that the disturbance is not entirely rejected by the minimal realization design as there is a sinusoidal residual in the error signal. In contrast, the NMSS design achieves this requirement (with only small fluctuations around zero). Figure 9 shows the errors in response to a step disturbance, the variations for the NMSS design are much smaller in magnitude.

More quantitative measures for the performance improvement delivered by NMSS realization are given by computing the mean squared error (18). Table I, where MR denotes minimal realization, summarizes this data for the six cases considered. All the experimental results conclude that the NMSS design provides much better closed-loop control performance in reference following and disturbance rejection. This performance improvement is significant as the mean squared error, denoted by ER_{per} in the last column of the table, is reduced by at least 80 percent for all the cases. In summary, the closed-loop performance of the minimal state-space realization deteriorates because an observer is required to estimate the state variables and hence introduces additional dynamics into the repetitive control system.

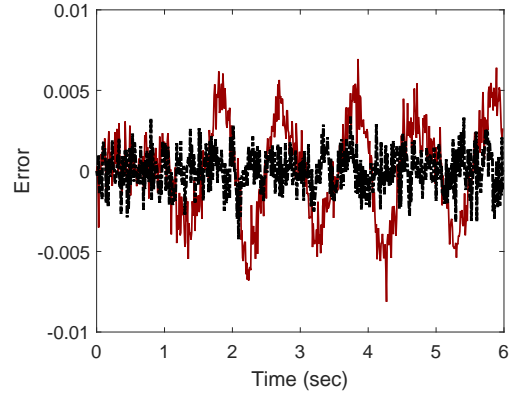


Fig. 7 The errors for reference tracking with no constraints.

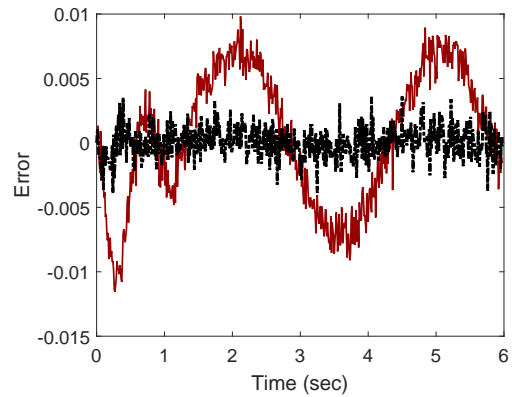


Fig. 8 Errors for a sinusoidal disturbance.

VI. CONCLUSIONS AND DISCUSSIONS

This paper has developed a disturbance observer-based repetitive control system using a non-minimal state-space realization. Control system design then becomes two simple yet independent tasks: first, designing a non-minimal state feedback control; second, designing a disturbance observer that will embed the characteristics of the disturbance signal or the reference signal into the control algorithm. The new design has been extensively evaluated using a gantry robot facility, including a detailed comparison with a repetitive control design based on a minimal state-space model design. These experiments demonstrate that the new design has significant advantages over alternatives both in design and implementation simplicity and performance.

REFERENCES

- [1] L. Ljung, *System Identification: Theory for the User*. Prentice-Hall, Englewood Cliffs, New Jersey, 1999.
- [2] T. Soderstrom, *Errors-in-Variables Methods in System Identification*. Springer, 2018.
- [3] P. C. Young, *Recursive Estimation and Time-series Analysis: an Introduction for the Student and Practitioner*, Springer-Verlag, Berlin, 2011.
- [4] C. Wang and P. Young, "Direct digital control by input-output, state variable feedback: theoretical background," *International Journal of Control*, vol. Vol.747, pp. 97–109, 1988.

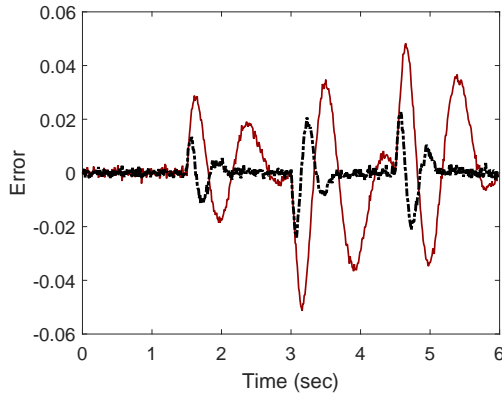


Fig. 9 Errors for a step disturbance.

Exper.	MR.	NMSS.	ERper
Ref. tracking	8.5×10^{-6}	1.5×10^{-6}	82.1
Ref. tra. with const.	9.1×10^{-6}	1.4×10^{-6}	83.9
Sinus. dist.	2.6×10^{-5}	1.4×10^{-6}	94.5
Sinus. dist. with const.	2.9×10^{-5}	4.4×10^{-6}	84.6
Step disturbance	3.3×10^{-4}	3.2×10^{-5}	90.0
Step disturbance with const.	7.3×10^{-4}	1.3×10^{-4}	81.7

TABLE I: Mean squared errors for the minimal and non-minimal realizations.

- [5] C. J. Taylor, P. C. Young, and A. Chotai, *True Digital Control: Statistical Modelling and Non-minimal State Space Design*. John Wiley & Sons, 2013.
- [6] L. Wang and P. C. Young, "An improved structure for model predictive control using non-minimal state space realisation," *Journal of Process Control*, vol. 16, pp. 355–371, 2006.
- [7] L. Wang, *Model Predictive Control System Design and Implementation using MATLAB*. Springer-Verlag, 2009.
- [8] B. Francis and W. Wonham, "The internal model principle of control theory," *Automatica*, vol. 12, pp. 457–465, 1976.
- [9] S. Li, J. Yang, W. Chen, and X. Chen, "Generalized state observer based control for systems with mismatched uncertainties," *IEEE Transactions on Industrial Electronics*, vol. Vol.59, pp. 4792–4802, 2012.
- [10] J. Yang, S. Li, and W. Chen, "Nonlinear disturbance observer-based control for multi-input and multi-output nonlinear systems subject to mismatching conditions," *International Journal of Control*, vol. Vol.85, pp. 1071–1082, 2012.
- [11] S. Li, J. Yang, W. Chen, and X. Chen, *Disturbance Observer-based Control: Methods and Applications*. CRC Press, 2014.
- [12] W.-H. Chen, J. Yang, L. Guo, and S. Li, "Disturbance-observer-based control and related methods: an overview," *IEEE Transactions on Industrial Electronics*, vol. 63, no. 2, pp. 1083–1095, 2016.
- [13] S. Komada, M. Ishida, K. Ohnishi, and T. Hori, "Disturbance observer-based motion control of direct drive motors," *IEEE Transactions on Energy Conversion*, vol. 6, no. 3, pp. 553–559, 1991.
- [14] E. Schrijver and J. van Dijk, "Disturbance observers for rigid mechanical systems: equivalence, stability and design," *Journal of Dynamic Systems, Measurement, and Control*, vol. Vol.124, pp. 539–548, 2002.
- [15] W.-H. Chen, D. J. Ballance, P. J. Gawthrop, and J. O'Reilly, "A nonlinear disturbance observer for robotic manipulators," *IEEE Transactions on industrial Electronics*, vol. 47, no. 4, pp. 932–938, 2000.
- [16] Q. W. Jia, "Disturbance rejection through disturbance observer with adaptive frequency estimation," *IEEE Transactions on Magnetics*, vol. 45, no. 6, pp. 2675–2678, 2009.
- [17] E. Sariyildiz and K. Ohnishi, "Stability and robustness of disturbance-

observer-based motion control systems," *IEEE Transactions on Industrial Electronics*, vol. 62, no. 1, pp. 414–422, 2015.

- [18] C. Bohn, A. Cortabarría, V. Härtel, and K. Kowalczyk, "Active control of engine-induced vibrations in automotive vehicles using disturbance observer gain scheduling," *Control Engineering Practice*, vol. 12, no. 8, pp. 1029–1039, 2004.
- [19] M. Bodson, "Rejection of periodic disturbances of unknown and time-varying frequency," *International Journal of Adaptive Control and Signal Processing*, vol. 19, no. 2-3, pp. 67–88, 2005.
- [20] M. T. White, M. Tomizuka, and C. Smith, "Improved track following in magnetic disk drives using a disturbance observer," *IEEE/ASME Transactions on Mechatronics*, vol. 5, no. 1, pp. 3–11, 2000.
- [21] Q. Zheng and M. Tomizuka, "A disturbance observer approach to detecting and rejecting narrow-band disturbances in hard disk drives," in *Advanced Motion Control, 2008. AMC'08. 10th IEEE International Workshop on*. IEEE, 2008, pp. 254–259.
- [22] R. Madoński and P. Herman, "Survey on methods of increasing the efficiency of extended state disturbance observers," *ISA transactions*, vol. 56, pp. 18–27, 2015.
- [23] L. B. McNabb, L. Wang, and B. McGrath, "Integrated approach to design and implementation of a single phase current regulator with anti-windup mechanism," *IEEE Transactions on Industrial Informatics*, vol. 17, no. 2, 2020, pp. 1231–1243.
- [24] L. Wang, J. Mishra, Y. Zhu, and X. Yu, "An improved sliding mode current control of induction machine in presence of voltage constraints," *IEEE Transactions on Industrial Informatics*, vol. 16, no. 2, 2019, pp. 1182–1191.
- [25] L. Wang, C. T. Freeman, and E. Rogers, "Repetitive-predictive control system with constraints: design and implementation," *Journal of Process Control*, vol. 23, pp. 956–967, 2013.
- [26] B. D. O. Anderson and J. M. Moore, *Optimal Filtering*. Prentice-Hall, Englewood Cliffs, New Jersey, 1979.